2013

Beach response to a sequence of extreme storms

Coco, Giovanni

Coco, G., et al., Beach response to a sequence of extreme storms, Geomorphology (2013), http://dx.doi.org/10.1016/ j.g
http://hdl.handle.net/10945/41277

Geomorphology xxx (2013) xxx–xxx

Contents lists available at ScienceDirect

Geomorphology

journal homepage: www.elsevier.com/locate/geomorph

Beach response to a sequence of extreme storms

Giovanni Coco [a,*], N. Senechal [b], A. Rejas [b], K.R. Bryan [c], S. Capo [b], J.P. Parisot [b], J.A. Brown [d], J.H.M. MacMahan [d]

[a] National Institute of Water and Atmospheric Research, Hamilton, New Zealand
[b] Bordeaux University, UMR CNRS 5805-EPOC, Talence, F-33405, France
[c] Dpt. of Earth and Ocean Sciences, University of Waikato, Hamilton, New Zealand
[d] Nearshore Processes Laboratory, Naval Postgraduate School, Monterey, USA

ARTICLE INFO

Article history:
Received 8 February 2013
Received in revised form 22 August 2013
Accepted 24 August 2013
Available online xxxx

Keywords:
Nearshore
Storm
Beach erosion
Morphodynamics
Beach survey, Beach recovery

ABSTRACT

A sequence of daily beach surveys acquired over one month covering an area larger than 100,000 m^2, was analyzed to study morphological changes resulting from a cluster of storms. The beach response was highly variable in both the cross- and alongshore. A cumulative storm effect was not observed, despite one storm being characterized by a 10-year return period that had significant wave height (H_s) of 8.1 m and a peak wave period (T_p) of 17 s. Instead, storms that can potentially cause significant erosion in terms of H_s had a limited effect on the morphology because the large wave height was coupled to either neap tides, normally-incident short-waves ($f > 0.04$ Hz), or low levels of infragravity ($0.004 < f < 0.04$ Hz) energy. Multiple linear regression analysis shows that volumetric changes in the upper part of the beachface are explained by offshore wave characteristics (period, height and direction), tidal range or by infragravity energy in the inner surf zone (assessed using pressure and velocity measurements). The results indicate that it is not possible to scale-up single-storm erosion studies into predictions of cluster-storm erosion.

1. Introduction

Long-term recession is a common feature of shorelines worldwide (e.g., Bird, 1985; Komar, 1998). Short-term recession can be traced to anthropogenic effects (e.g., Frihy and Komar, 1993), while climate change or variations in sediment supply are potentially the main driver of long-term erosion (Stive, 2004; Zhang et al., 2004). These recession patterns are the result of cross- and alongshore gradients in sediment fluxes, which cause sediment redistribution between the onshore and offshore areas, between up and down the coast, and ultimately induce net erosion and accretion. The intrinsic difficulties in estimating sediment transport due to the presence of thresholds, non-linearities, bedforms, and different modes of transport make the up-scaling from short-term (~minutes) and small-scale (~centimeters) predictions of sediment transport to long-term (>days) and large-scale (~kilometers) predictions of beach evolution an extremely challenging exercise. Depending on the magnitude of the forcing conditions, the role of waves can quickly change from accretive small wave conditions to erosive storm wave conditions. Although simplistic, this approach holds also when describing subaqueous sandbars that tend to move slowly onshore during calm, accretive conditions and more rapidly migrate offshore during stormy, erosive conditions (Gallagher et al., 1998; Plant et al., 2006). However, such simplistic models do not provide the level of detail needed by planners to define coastal hazard zones or by engineers to estimate fill quantities needed for post-storm re-nourishment.

Studies have shown that shorelines can partially recover from storm-induced erosion and that the initial recovery can be extremely fast. For example, Wang et al. (2006) showed that substantial beach recovery in the form of re-establishing the pre-storm beachface slope and berm occurred within 90 days. Even more impressively, Birkemeier (1979) showed that up to half of the sand eroded during the storm was recovered within one day of the storm. On the other hand, a full recovery from major storms can also last for years, especially if erosion of the dunes backing the beach has occurred (Thom and Hall, 1991). In fact, the 'vulnerability' of a beach, intended as the potential of a beach to be affected by a major storm, depends on the balance between storm frequency and recovery rates. Studies of beach vulnerability depend on understanding the role of dunes that act as sediment reservoirs, sandbars that shelter the beach from wave action, and the three-dimensional (3D) response of the whole coastal system.

The difficulty in collecting adequate datasets makes the study of the role of storms on long-term beach change challenging (Zhang et al., 2002; Anderson et al., 2010) with most studies focusing on detailed measurements of fast-scale hydrodynamic and sediment transport processes at a selected location (e.g., Aagaard et al., 2005), or on the analysis of beach profiles which are usually sparse in time (e.g., Almeida et al., 2012). Datasets with adequate resolution in both time and space are uncommon, and even fewer studies have addressed the effect of 'clusters' of storms on beach response (Birkemeier et al., 1999; Ferreira, 2006). Lee et al. (1998) and Birkemeier et al. (1999) analyzed long-term beach profile surveys from Duck (North Carolina, USA) and concluded

* Corresponding author at: Environmental Hydraulics Institute 'IH Cantabria', Universidad de Cantabria, c/Isabel Torres 15, 39011, Santander, Spain.
E-mail address: cocog@unican.es (G. Coco).

0169-555X/$ – see front matter © 2013 Elsevier B.V. All rights reserved.
http://dx.doi.org/10.1016/j.geomorph.2013.08.028

that a sequence of storms has a 'cumulative' effect on beach erosion, and if the beach has no time to recover, clusters of storms have an effect comparable to that of a less frequent and more energetic storm with respect to both intensity and storm duration. Numerical modeling studies show that wave chronology also affects beach profile evolution (Southgate, 1995; Ferreira, 2005). These findings need more corroboration by comprehensive observational studies over various beach types before they can be translated into beach management practices.

In the present work, we discuss whether the response to multiple storm events is equal to the linear sum of the effect of each storm or whether the last storm results in increased or decreased erosion. Both hypotheses are viable and in this context recent data-driven models have shown that shoreline erosion tends to diminish if erosive conditions are maintained (Yates et al., 2009). At the same time, because of the difficulty in collecting an appropriate dataset, little is known about the alongshore variability in beach response to storms. Here, we use detailed topographic surveys that were obtained daily over an area of 100,000 m^2 for 30 days and concurrent hydrodynamic measurements to describe the beach response of volumetric erosion and alongshore morphologic evolution caused by a series of storms. Each storm response is characterized as a function of its offshore and inner surf zone hydrodynamic characteristics estimated from an offshore directional buoy and a current meter located in the surf zone. Finally, we take advantage of the fortuitous sequence of extreme storms to analyze and discuss the beach response to extreme storms of varying duration and magnitude.

2. Field site

A surf zone field experiment was performed at Truc Vert beach, located south of Bordeaux, France, in close proximity to the Arcachon lagoon (Fig. 1) in March to April 2008 (Senechal et al., 2011a). The beach is a typical representation of the south Atlantic coastline of France, which is characterized by an undisturbed sandy shoreline and by well-developed aeolian dunes (Senechal et al., 2009). Truc Vert beach is characterized by the presence of two sandbars, one subtidal and one intertidal, whose shape ranges from linear to the more commonly-observed crescentic shape. The inner sandbar is usually more dynamic with the presence of well-formed rip channels (Castelle et al., 2007). The mean grain-size of the beachface is 0.35 mm. Truc Vert is a macro-tidal beach with a tidal range varying from 1.5 m during neap tides to 5 m during spring tides. The mean annual offshore significant wave height (H_s) and period (T_p) are 1.4 m and 6.5 s (Butel et al., 2002), and events that are characterized by $H_s > 4.1$ m and $T_p > 10.1$ s are classified as storms (Le Cozannet et al., 2011).

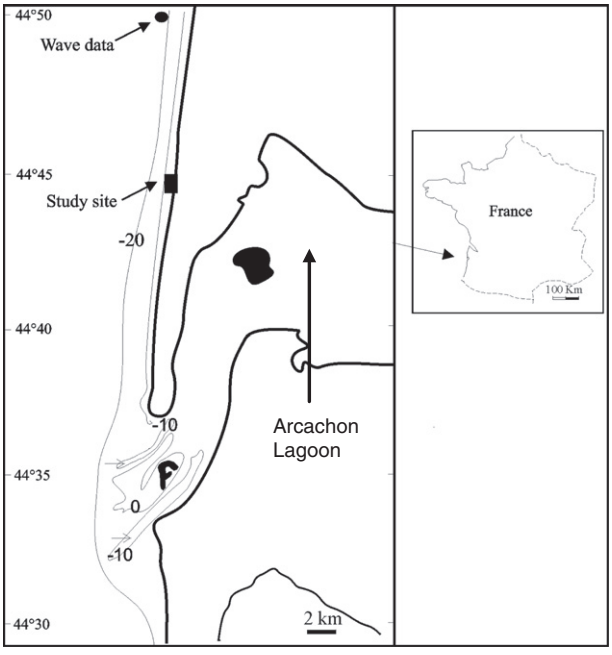

Fig. 1. Map of the Truc Vert study site.

3. Methods

Twenty nine topographic surveys were conducted daily around low tide from March 4 to April 8, 2008, using four Differential GPSs (DGPSs) with horizontal and vertical errors of less than 0.05 m. One DGPS was positioned on an all-terrain vehicle and three DGPSs were mounted to human walkers to survey the inner surf zone, swash zone, and the dunes. Cross-shore beach profiles were measured from the dune to the edge of the swash with an alongshore spacing of 20 m (an average of 50 profiles was obtained during each survey). Additional information about the surveying technique and the errors associated with the beach survey are described in Parisot et al. (2009). Two larger offshore bathymetric surveys were performed by the SHOM (Service Hydrographique et Oceanographique de la Marine) on February 14 and April 7–9 (Fig. 2). In addition, images from a two-camera system were collected at 2 Hz from March 8 to April 7 to infer the position and dynamics of the subaqueous sandbars (results are presented in Almar et al., 2010).

H_s, T_p, and wave direction (θ_p) were measured every 30 min by a directional wave buoy located in 20 m water depth offshore of the area surveyed. Water levels were extracted every 30 min from a regional tidal model that was corrected with a tide gauge in the Arcachon lagoon. In order to analyze temporal variations in the offshore wave climate and so in the amount of breaking-related dissipation, we used the Iribarren number which is defined as:

$$\zeta = \tan\beta / \sqrt{H_0/L_0}, \quad (1)$$

where tan β is the beach slope, calculated as the alongshore average of the cross-shore slope between 1 and 3 m contours, L is the wave length, and the subscript 0 refers to deep water conditions.

Surf zone hydrodynamics were measured throughout most of the experiment using a collocated pressure (p) sensor and horizontal electromagnetic current meter that measured cross- (u) and alongshore (v) velocity components, referred to as a PUV sensor. The location of this array is shown in Fig. 2. Using these measurements, we calculated 3-h means of p, u, and v for different frequency bands: very low frequency (vlf, $0.0005 < f < 0.004$ Hz), infragravity (ig, $0.004 < f < 0.04$ Hz), and swell (sw, $0.04 < f < 0.2$ Hz). Instrument heights off the bed were collected for 30 days and are accounted for when calculating wave properties and the total water depth.

4. Results

4.1. Hydro- and morphodynamic changes

The pre-experiment bathymetry showed three-dimensionality of the outer bar characterized by a crescentic shape with an alongshore horn spacing of around 600 m (Fig. 2, left panel). Similar to the observations of Ruessink et al. (2007), the pattern of the outer bar, although subdued, is reflected onto the morphology of the inner bar (Fig. 3, top panel). A cross-correlation between the detrended vertical elevations along the outer and inner bar measured around cross-shore positions 650 and 250 m resulted in a low, but 95% statistically significant, regression coefficient ($r = 0.4$, $p < 0.05$) at zero spatial lag. In the cross-shore direction, beach profiles display different characteristics depending on their alongshore position. Cross-shore profiles corresponding to the horns of the crescents (Fig. 4) show an asymmetric outer sandbar with a crest that is much shallower than the one corresponding to profiles at the bays of the crescents. Following the sequence of storms (Fig. 2, middle panel), the outer sandbar still displayed a strong crescentic pattern with

Please cite this article as: Coco, G., et al., Beach response to a sequence of extreme storms, Geomorphology (2013), http://dx.doi.org/10.1016/j.geomorph.2013.08.028

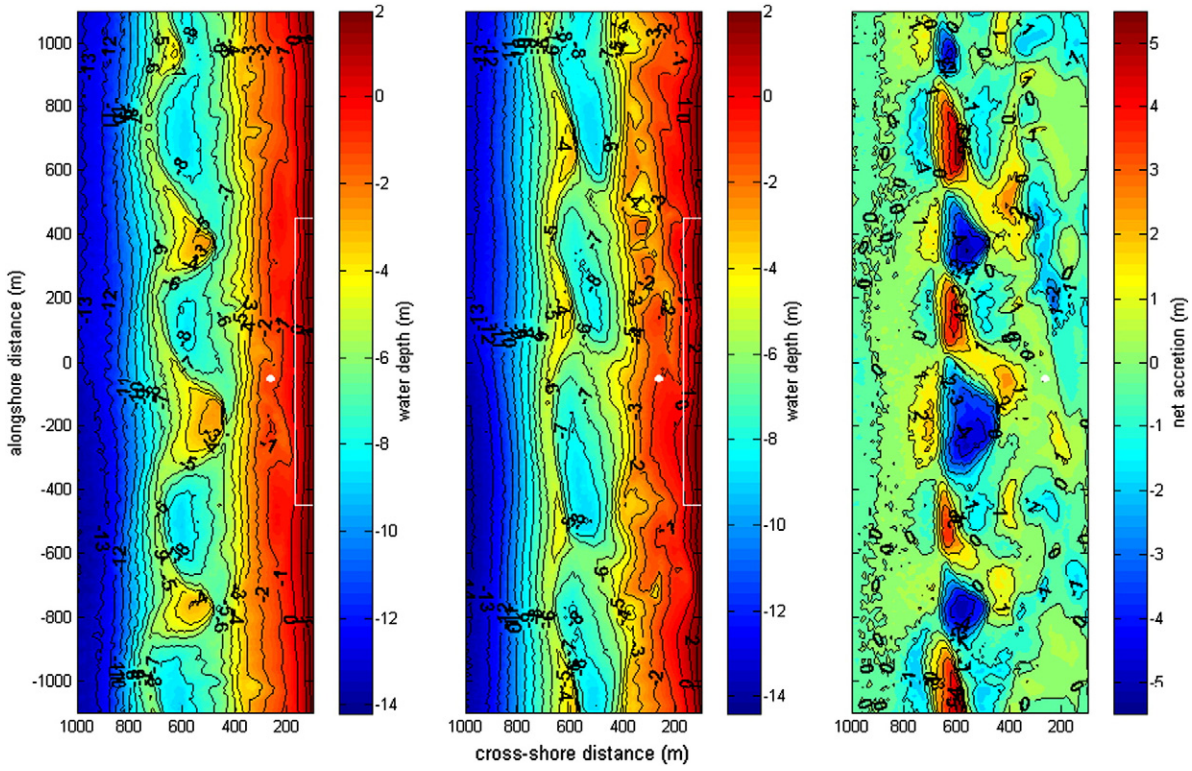

Fig. 2. Contours of beachface and bathymetry of Truc Vert beach as a function of alongshore and cross-shore position (offshore is positive to the left, north is towards the top of the panels). Panels show the survey performed on February 14 (left panel), the survey of April 7–9 (middle panel) and the net morphological change (right panel). Contour lines are plotted with 1 m spacing. A colorscale of MSL elevation is plotted to the right. The white-lined box indicates the area over which daily surveys were completed. The white dot indicates the location of the inner surf zone sensor.

an alongshore horn spacing of 600 m. The inner sandbar still displayed a number of undulations reflecting the alongshore pattern of the outer sandbar. The cross-correlation was also statistically significant at 95%, but negative ($r = -0.4$) with a spatial lag of 100 m, implying that the sandbar positions are out of phase (Fig. 3 bottom panel).

Four large storms occurred during the experiment (Fig. 5). The first storm (S1, March 3 to 5) peaked around low tide of March 4 during neap tides with a maximum $H_s = 6.3$ m, $T_p = 15$ s, and $\theta_p = 14°$. Unfortunately, this storm took place just before the onset of the beach profile survey campaign and its effects cannot be assessed.

The second storm (S2, March 9 to 12) peaked during the night of March 10 with a maximum $H_s = 8.2$ m, $T_p = 16$ s, and $\theta_p = 10°$ and occurred during spring tides. The S2 estimated return period for this storm is 10 years (Ardhuin, pers. comm.). At the peak of S2, the tidal level was around 1 m above mean sea level (MSL). The PUV sensor measured a large wave setup (Fig. 6b), indicating that the large offshore

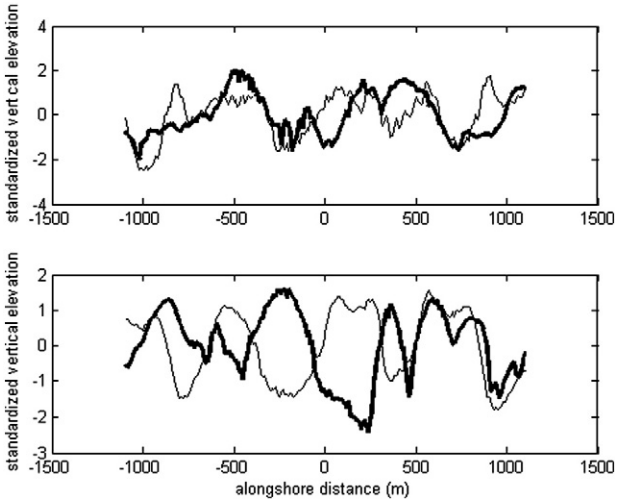

Fig. 3. Standardized vertical elevations along the outer (thick line) and inner (thin line) bar at the beginning (February 14, top panel) and the end (April 7–9, bottom panel) of the field campaign. Alongshore transects of beach elevations representative of the outer and inner bar were measured around cross-shore positions 650 and 250 m.

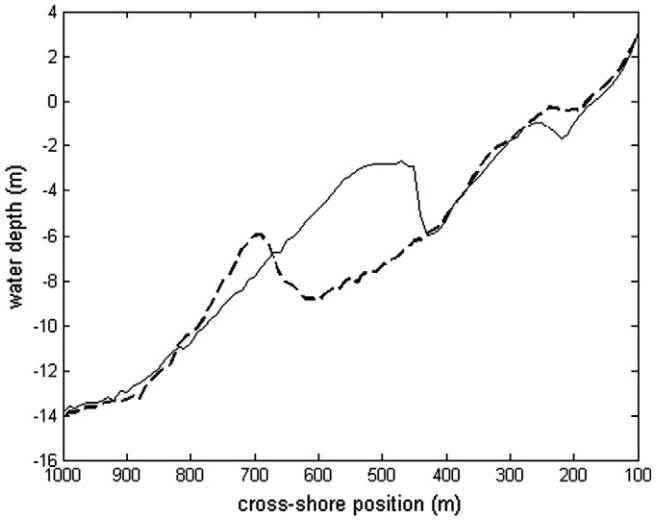

Fig. 4. Cross-shore beach profiles at alongshore position −150 (dashed line) and +200 m (continuous line), which correspond to a crescent bay and horn, respectively (see Fig. 2). Profiles are derived from the survey performed on February 14 (see Fig. 2, left panel).

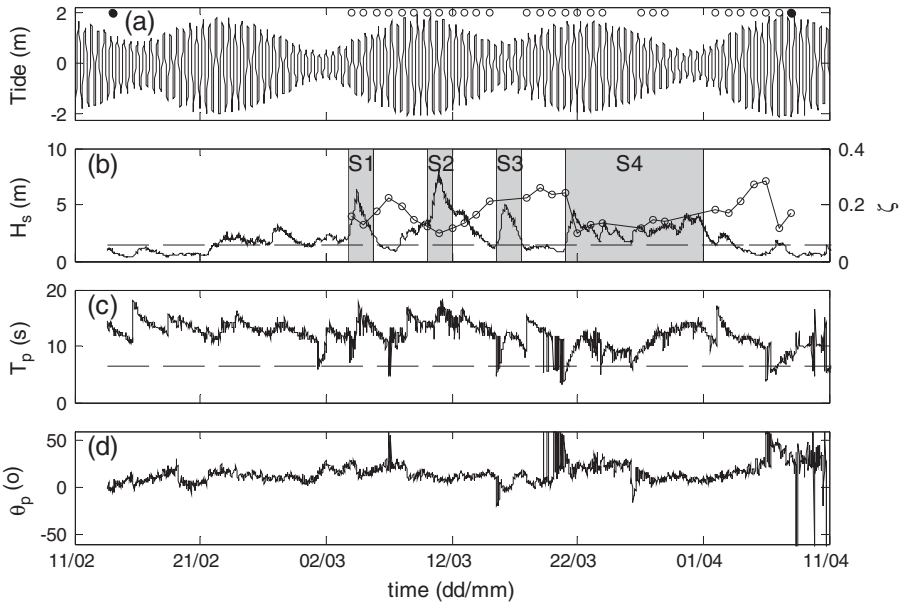

Fig. 5. (a) Water level relative to MSL, (b) offshore H_s (continuous line) and Iribarren number (circles linked by a continuous line), (c) offshore T_p and (d) offshore wave direction. Open circles in (a) represent dates when beach surveys were conducted and filled circles indicate dates when large-scale bathymetric surveys were conducted. Horizontal dashed lines in (b) and (c) indicate mean annual values. Shaded areas in (b) indicate the storms S1, S2, S3, and S4.

waves dissipated most of their energy before reaching the inner surf zone (Fig. 6a, H_s has decreased to about 1 m). The wave heights at the PUV sensor modulated with the tides, and were affected by depth-limited breaking. During the onset of S2, p_{ig} increased rapidly and was a factor of two larger than p_{sw} before the peak of the storm and the related instrument failure (Fig. 6d). The p_{ig}/p_{sw}, p_{vlf}/p_{sw}, u_{ig}/u_{sw}, v_{ig}/v_{sw} ratios were larger during this storm than at any other time during the experiment (Fig. 6d–f). At this stage of the experiment, the PUV sensor was located near a rip channel, which might contribute to the large increase of signals (pressure and velocity) in the infragravity and very low frequency bands. Both u_{ig}/u_{sw} and v_{ig}/v_{sw} were tidally modulated (Fig. 6e,f) and primarily offshore- and southward-directed. Power outage during the height of the storm (March 11 to March 13) prevents further insights. The large waves and super-elevation of the mean water level due to the spring tides and storm-induced setup during S2 caused strong erosion of the upper part of the beachface above the 4 m contour line and removed the alongshore morphological variability in the surf zone (Fig. 7a–c). The two rip channels that were present on March 7 were infilled during the storm, with strong localized accretion of up to 0.5 m measured at the most offshore extent of the rip channel. Sediment from the upper beachface was transported towards the 2 and 4 m contours, where moderate accretion is observed. Below the 2 m level, apart from the infilling of the rip channels, erosion dominates as one would expect for a major storm event. The net accretion/erosion patterns occurring

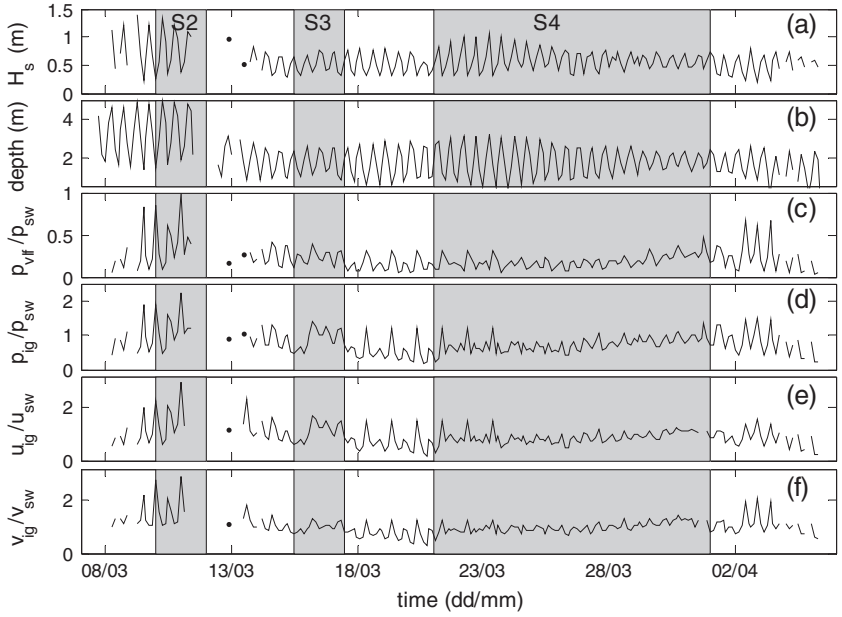

Fig. 6. PUV measurements of (a) surf zone wave height, (b) water depth, ratio between (c) p in the vlf and sw bands, (d) p in the ig and sw bands, (e) u in the ig and sw bands, (f) v in the ig and swl bands. Shaded, grey areas indicate the occurrence of the storms (S2–4).

Please cite this article as: Coco, G., et al., Beach response to a sequence of extreme storms, Geomorphology (2013), http://dx.doi.org/10.1016/j.geomorph.2013.08.028

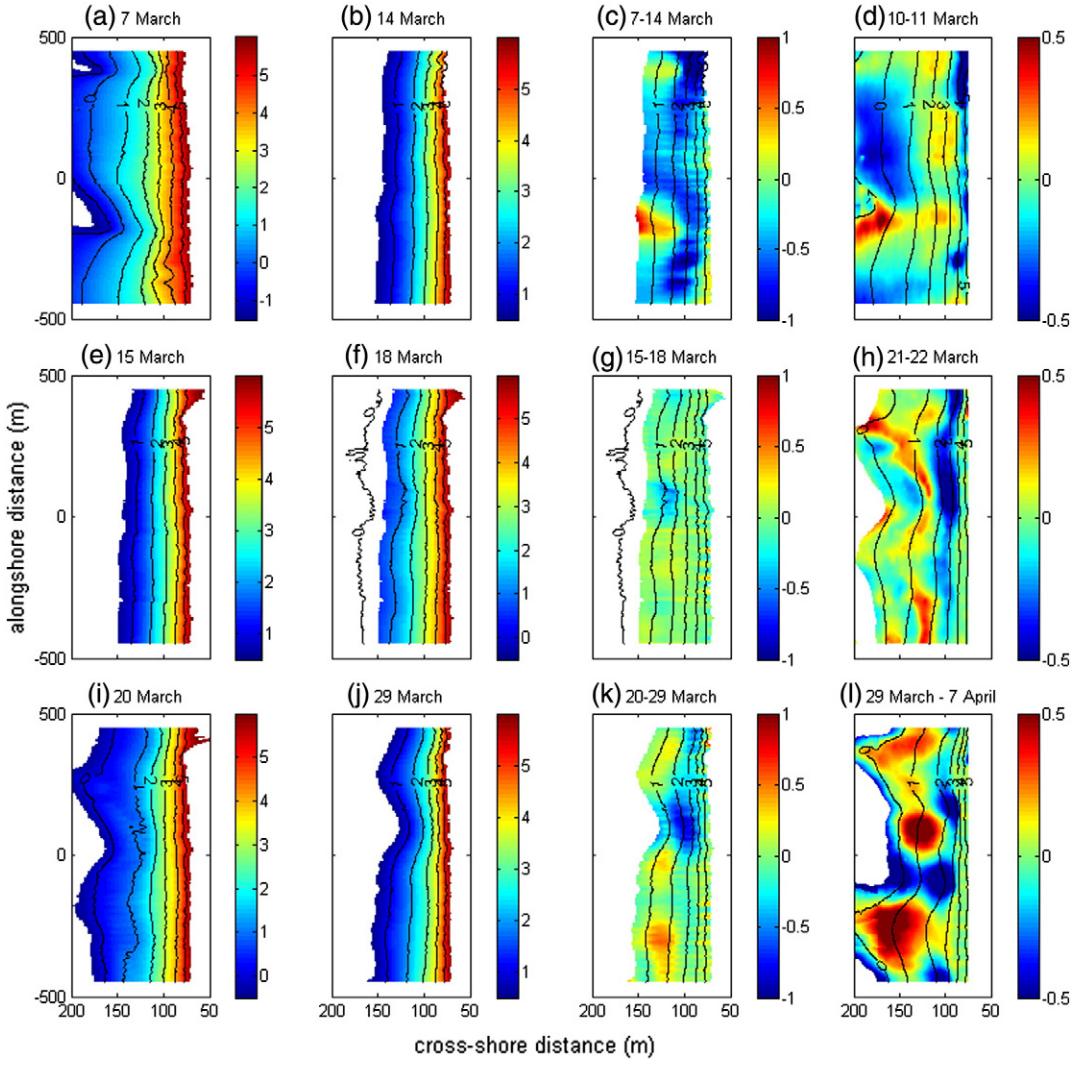

Fig. 7. Contours of beachface surveys (elevation relative to mean sea level) as a function of alongshore and cross-shore position (offshore is to the left, north towards the top of the subplots) for each of the three surveyed storms (S2, S3 and S4). Top, middle and bottom row show the topography before (first column, subplots a, e, i) and after (second column, subplots b, f, j) S2, S3 and S4 respectively. Subplots in the third column (c, g, k) show the net morphological change (contours are from the later of the beach surveys) where red indicates accretion and blue indicates erosion. Subplots in the fourth column show net morphological change between the surveys of (d) March 10 and 11, (h) March 21 and 22, (l) March 29 and April 7. Contours are from the last of the beach surveys (March 11, March 22, and April 7). The survey dates are on top of each panel. Contour lines are plotted at 1 m spacing. The coordinate system is the same as in Fig. 2. Colorscales of elevation and elevation differences are plotted to the right.

around the peak of S2 between March 10 and 11 (Fig. 7d) resulted in strong alongshore and cross-shore variability in erosion and deposition. As shown by video images (see Fig. 8), the offshore sandbar responded to S2 by changing configuration from crescentic to linear (see also Almar et al., 2010). This type of response is consistent with observations collected at other beaches globally (van Enckevort et al., 2004).

The third storm (S3, March 15 to 17) peaked on March 16, just 4–5 days after the peak of S2 (Fig. 5) and occurred during −1 m low tide (neap tides). The maximum offshore H_s was 5 m, which is more than 3 times the mean annual value, waves were near normally incident ($\theta_p = -2°$), and $T_p = 12$ s which was lower compared to the previous storm. The increase in p_{ig}/p_{sw}, p_{vlf}/p_{sw}, u_{ig}/u_{sw}, v_{ig}/v_{sw} was marginal, especially when compared to the rapid increase observed during S2 (Fig. 6c–f). Despite H_s reaching 5 m at the peak of S3, the beachface experienced only moderate erosion (Fig. 7e–g).

After a period of small waves (offshore $H_s < 1.5$) from March 18 to 20, a fourth storm (S4) occurred (Fig. 5). Strictly speaking, S4 could not be classified as a storm in terms of offshore wave height (Le Cozannet et al., 2011) which was not extreme. On the other hand, the duration of consistently large waves and their effect on beach morphodynamics make this event comparable to an extreme storm. In fact for about 10 days (from March 21 to April 1), H_s was above the mean annual value with peaks above 4 m. More specifically, the mean H_s for S4 was 2.9 m, which is more than twice the mean annual value, and T_p reached 15 s with a mean value of 11 s. The largest H_s occurred at the beginning (March 21) and at the end (March 30) of the S4 event. Owing to the 10-day storm duration, water levels changed from spring to neap tides. With respect to the angle of wave approach, from March 21 to 26, waves approached the beachface from the north-west (mean angle around 20°) while during the rest of the storm the mean angle decreased to about 10°. The PUV (Fig. 6c–f) shows a progressive increase of the infragravity component of the pressure signal throughout the storm and by March 30 the magnitude of the infragravity and swell components are comparable.

Beachface response to this storm differed over time. At the beginning of S4 the beachface eroded between the 2 and 4 m contours, while the lower part of the beach underwent either accretion or minor erosion (see changes occurring on the upper part of the beach between 21 and 22 March, Fig. 7 h). Beachface response was also variable in the alongshore as evidenced by an increase in the three-dimensionality around

Please cite this article as: Coco, G., et al., Beach response to a sequence of extreme storms, Geomorphology (2013), http://dx.doi.org/10.1016/j.geomorph.2013.08.028

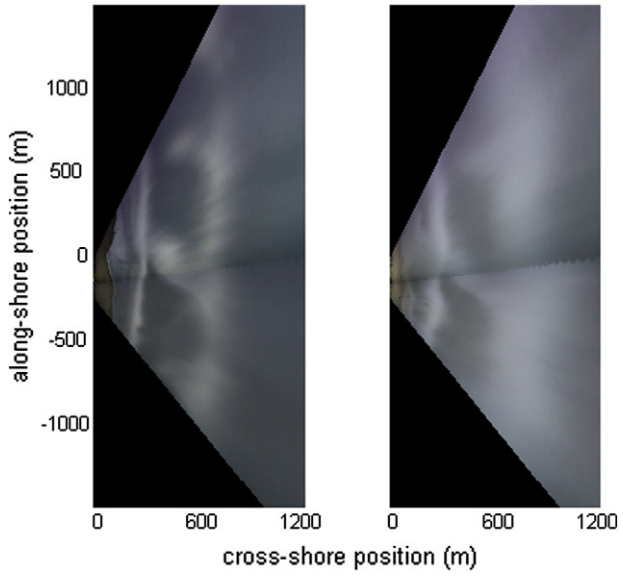

Fig. 8. Orthorectified images of Truc Vert beach on (left panel) March 8 and (right panel) March 12.

the 0 m contour, where a shoreline sandwave developed with an alongshore spacing between horns of ~400 m. The simultaneous presence of large waves and a large angle of wave approach (around 20°) resulted in a migration of the sandwave. Fig. 7 h shows that most of the accretion around the 0 m contour was on the southward side of the offshore-protruding parts of the sandwave. Overall, the sandwave migrated southward (positive values of the alongshore position) about 100 m during the period between March 18 and 24 (value estimated using cross-correlation analysis, Fig. 9). Between March 24 and 29, offshore H_s remained large but never exceeded 4 m, tidal range decreased and the wave field became more shore-normal. By March 28, $\theta_p < 10°$ marking the beginning of an accretionary phase for elevations below 1 m which accelerated strongly at the end of March when wave height dropped below 1 m. At the end of the survey campaign (April 7), the beachface (Fig. 7 l) and the shape of the sandbars (Fig. 3) develop a three-dimensionality. The end of the survey campaign also coincided with strong erosion of the upper part of the beach. This event was not associated with large waves (H_s ~ 1.4 m) but rather with the combination of spring tides and large θ_p (see Fig. 5 around April 7), and the increase in energy towards lower frequencies (Fig. 6).

Alongshore variability across the beachface was examined to explore the changes from alongshore uniform to variable and is shown in Fig. 10. S2 resulted in large erosion above the 1 m contour line with sand being transported during the onset and the peak of the storm towards lower beach levels, where high amounts of alongshore variability were related to the presence of a large rip channel. Variability decreased during the decaying phase of the storm. This is particularly evident for isolines from 0 to 2 m where the reduction in standard deviation is statistically significant (F-test $p < 0.05$) and equal to a factor of three. Smaller reductions in the standard deviation are observed on the upper part of the beach. At the same time, the lower beach contours (between 0 and 1 m) showed large erosion and both migrated onshore by up to 10 m. Fig. 10 also shows erosion of the embryo dunes (contour lines above 3 m), which resulted from the elevated water levels driven by the occurrence of spring tides, the setup associated with the storm, and the large amount of infragravity energy present in the incoming wave field (Fig. 6). Consistent with these findings, swash time series measured during the same storm were dominated by energy at infragravity frequencies (Senechal et al., 2011b). Surveys performed near the onset and after the peak of S3 confirm the limited effect of this storm on beach erosion with beach three-dimensionality only increasing slightly. Finally, the long duration and smaller magnitude of S4 resulted in erosion of the upper part of the beach with sediment likely to be transported to offshore locations. At the same time, the alongshore variability increased in the lower part of the beachface below isoline 2.5 m and is statistically significant (F-test $p < 0.05$), which is an indication that the large-scale alongshore pattern is beginning to redevelop during later stages of S4 (e.g., March 28) and becomes extremely large when calm conditions are re-established (e.g., April 4).

The cross-shore beach profile evolution provides insight into mechanisms of beachface erosion and sediment transport. Two distinct erosive events are observed (Fig. 11). The first is associated with the highest magnitude storm, S2 (Fig. 11a) and the second with very low waves and spring tides (April 5–7, Fig. 11b). The overall effect of S2 is uniform erosion across the beachface with the beach profile receding of about 5–10 m horizontally (Fig. 11a). In contrast, erosion can occur also when large waves are not present (Fig. 11b). Between April 5 and 7, H_s was

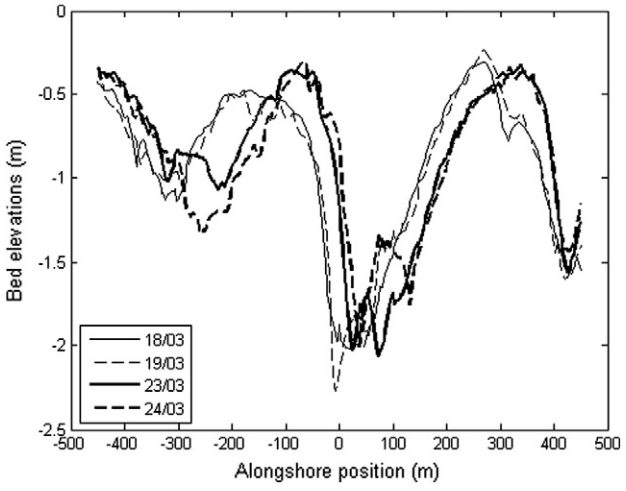

Fig. 9. Alongshore sandwave migration. Bed elevations as a function of alongshore position at cross-shore position of 200 m.

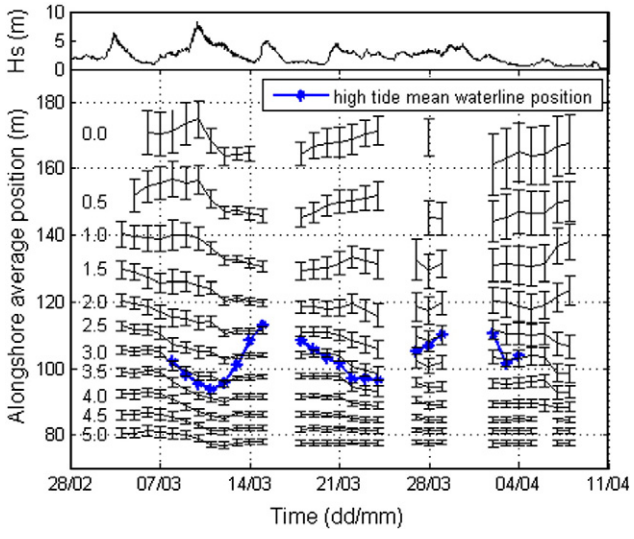

Fig. 10. Alongshore variability in beach response. Top panel: Offshore H_s. Bottom panel: Each black line represents the mean alongshore position for different contour lines (each contour line is labelled on the left). Vertical bars indicate the alongshore variability denoted by 1 standard deviation of the mean contour line position. Missing values indicate lack of data. The blue line indicates the high tide mean waterline position as measured from a pressure sensor on the inner sandbar. Offshore direction is upwards.

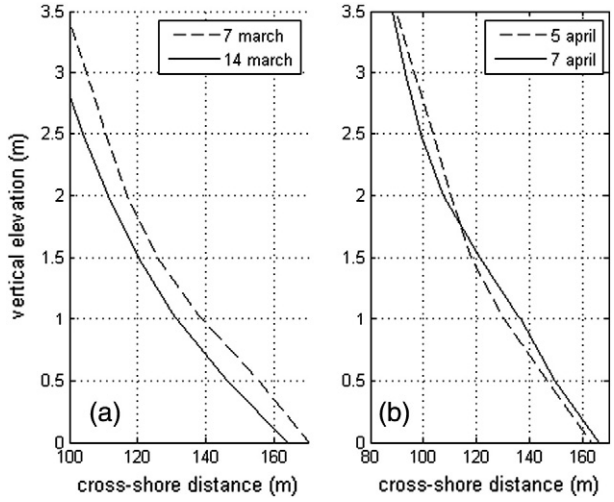

Fig. 11. Alongshore mean of cross-shore profiles before (dashed line) and after (continuous line) events characterized by (a) a storm and (b) a combination of spring tides and waves approaching with a large angle of approach.

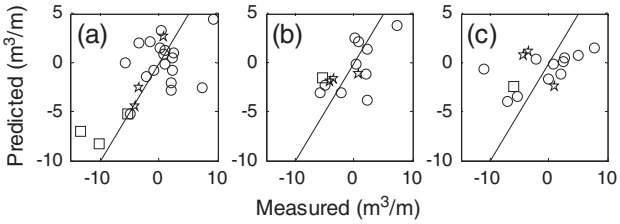

Fig. 12. Comparison between measured and predicted volumetric beach changes per unit of alongshore length in the upper (0 to 6 m) part of the beach using (a) offshore variables (wave height, peak period, angle of approach, tidal range) and inner surf zone measurements of (b) pressure and velocity in the ig band, and (c) pressure and velocity in the sw band. Squares refer to the changes occurring during S2, stars to the beginning of S4 and circles to all other available measurements.

~1 m but water levels were high due to spring tides and θ_p ~30–40°. This resulted in the transport of sediments from the upper to the lower part of the beachface with a nodal point around a vertical elevation just above 1.5 m (Fig. 11b).

4.2. Regression analysis

Offshore and inner surf zone hydrodynamic data are used to explain morphological changes throughout the experiment. Offshore variables considered in this study were H_s, T_p, θ, and, because of the large variations in water levels between spring and neap tides, we also included tidal range (TR) as a potential predictor of morphological change. Inner surf zone measurements considered were pressure and velocity at vlf, ig, and sw frequencies. Daily averages of these hydrodynamic variables over the day prior to each beach survey provided the best results, as opposed to using maximum values or squared and integrated values. Morphological change was quantified by integrating bed elevation differences between subsequent surveys within elevation ranges of −2 to 0 m and 0 to 6 m, and then dividing by the length of the beach. The selected ranges gave the best compromise between maximising the available data and providing insight on the physical processes.

The first step of the analysis involved regressing changes in beach elevation on offshore and inner surf zone variables separately. The correlations were not statistically significant in any of these cases so that, in order to assess the combined role of forcing variables, multiple linear regression analysis was needed. Beach changes between −2 and 0 m could not be significantly explained by any combination of offshore or inner surf zone variables. Above MSL, a multiple linear regression using offshore data provided statistically significant predictions for beach change ($r = 0.66$, $p < 0.05$, Fig. 12a). Beach changes above MSL were also explained using inner surf zone variables, including the ig proportion of the pressure and velocity fields ($r = 0.59$, $p < 0.05$, Fig. 12b). The vlf component (not shown) gave similar results to the ig component, however there was a lack of correlation ($r = 0.44$ but $p > 0.05$) between data at sw frequencies and beach changes (Fig. 12c). Regressions calculated between beach change and the Iribarren number (Battjes, 1974) or the distance between the shoreline and the inner sandbar (as calculated in Almar et al., 2010), both resulted in insignificant correlations.

5. Discussion

The large spatial extent (on average, 900 m in the alongshore and 150 m in the cross-shore) and long duration of the measurements allowed for a detailed quantification of morphological evolution over a sequence of extreme storms at Truc Vert beach. S2, which had the greatest H_s, caused large beachface erosion (~25 m^3/m) while S3 (maximum value of H_s was 5 m) caused only limited erosion (<2 m^3/m). The different response could be the result of a combination of factors, which are not easy to identify and separate. From a hydrodynamic perspective, the main factors included the limited increase in infragravity energy levels, near normally-incident waves, and concomitant occurrence of neap tides with a storm that peaked around low tide. Changes in the width of the surfzone and in offshore dissipation must have also played a role since H_s measured at the PUV sensor was as large as 1 m during S2 but it was about 0.5 m, i.e. not different from non-storm days, during the other storms (Fig. 6a). From a morphodynamic perspective, S2 might have caused so much erosion (and offshore sediment transport) that the response to this subsequent, smaller storm was minimal. The only erosive signature on the beachface was related to the development of a rip channel extending to the inner sandbar at alongshore position +50 m, while the rest of the beachface was characterized by moderate accretion or erosion. The outer bar was not active during S3 (no breaking was observed in correspondence of the sandbar crest). S4, which was characterized by smaller H_s than in S3, resulted in greater erosion (~6 m^3/m) than S3. During S4 erosion was concentrated on the upper part of the beach and was concomitant with the occurrence of spring tides. Tides per se are not a source of erosion but the occurrence of spring tides with extreme H_s (S2) or large θ_p (April 7 during S4) leads to the largest measured erosive events. Masselink et al. (2009) reported measurements of bed elevation changes across the swash zone during S4. The measurements were performed on a swash by swash basis and indicated that the presence of strong longshore currents was a primary cause of beachface erosion.

Measured erosion/accretion values are limited to the beachface and do not extend sufficiently far offshore to allow for a reliable assessment of sediment budget or to evaluate the relative role of cross-shore versus alongshore processes. Nevertheless, they do provide a reliable estimate of net changes occurring on the beachface as a result of the storms. Estimates of net sediment loss/gains between the pre- and post-experiment large-scale bathymetric surveys (Fig. 2) indicate that most of the sediment is redistributed across the nearshore region with a net loss of −0.24 m^3/m and −1.12 m^3/m for elevations between +6 and 0 m, and 0 and −8 m, respectively. This is only partly compensated by moderate accretion offshore of 1.11 m3/m between −8 and −12 m. The overall erosion is minor, with −0.25 m^3/m for elevations between +6 and −12 m.

An intriguing finding is the presence of periodic 3D features both at the beginning and end of the campaign (Figs. 2, 3). Despite the sequence of extreme storms, the length-scale of the alongshore pattern of the initial and final beach configuration is surprisingly similar suggesting that this is the natural state. Changes from 3D to 2D and then 3D again can be explained by the differences between the individual storms. S2 caused a decrease in alongshore variability and considerable erosion (e.g., Fig. 7),

Please cite this article as: Coco, G., et al., Beach response to a sequence of extreme storms, Geomorphology (2013), http://dx.doi.org/10.1016/j.geomorph.2013.08.028

consistent with existing observations of changes in sandbar configuration from 3D to alongshore uniform (van Enckevort et al., 2004). Conversely, beachface surveys performed during and after S4 (March 28 and April 7) revealed beachface accretion (>2 m^3/m) and the concurrent development of 3D morphology. S4 was characterized not only by smaller H_s and T_p, but also by a lower amount of ig and vlf energy, ignoring the period between April 2 and April 4 (Fig. 6). In terms of beach contours, the minimum value of alongshore standard deviation of elevation (a proxy for 2D morphology) occurred around March 14 after S2 (Fig. 10) and, despite the occurrence of S3, it increased to large values indicative of 3D morphology within 7–10 days. These results provide a tentative timescale for the return to 3D morphology. Unfortunately, the lack of subaqueous surveys prevents a definitive statement on the role of the offshore sandbar in providing a template to cause 3D morphology also in the inner sandbar and the shoreline (as shown in Castelle et al., 2010), and in accounting for exchanges of sediment between the outer and inner sandbar (Almar et al., 2010) which could ultimately affect the beachface. Overall, it appears that the development of 3D morphology is associated with calm/accretionary conditions, while 2D morphology results from stormy/erosive conditions (these conditions can not be uniquely defined as they are site-specific and depend on previous hydrodynamic conditions and current beach configuration).

The large-scale pre- and post-experiment surveys demonstrate that the length-scale of the beach surveyed is large enough to provide a good representation of the processes occurring over the long straight coast of Truc Vert beach. The morphodynamics of the large-scale alongshore pattern, a sequence of highs and lows typical of rip channel systems, is captured well by the surveys and, in agreement with the original work of Wright and Short (1984), shows the development/disappearance of alongshore periodicity as a result of the sequence in stormy/calm conditions (Fig. 3).

These results demonstrate that a sequence of extreme storms does not necessarily result in cumulative erosion and suggests that a cautionary approach to 'storm clustering' is needed. Our results support the suggestion (Birkemeier et al., 1999) that design storm conditions may need to be recomputed based on the frequency of storm sequences, as opposed to individual wave or storm conditions. However, defining precisely how sequences of storms should be combined is not clear as, for example, in our observations, one storm in the 'cluster' actually resulted in very limited net erosion. The concept of 'storm clustering' is usually based on offshore wave heights while the present study, using multiple linear regression, shows that in order to explain storm effects, one needs to also account for tidal levels, ig energy in the incoming wave field and wave direction and period. Also, any model trying to assess the role of 'storm clustering' should be able to account for the development or disestablishment of three-dimensionality in the surf zone as wave energy is not only used to generate 'net morphological change' but also to rearrange sediment in distinct shapes. Overall, in agreement with other studies (e.g. Russell, 1993), our analysis suggests that low-frequency energy, particularly that associated with ig waves during S2, is certainly a major factor in shaping the morphology during storms. Conversely, the role of vlf energy remains to be established.

It is likely that a more global approach that accounts for the possible detailed characteristics of each storm (H_s, T_p, θ_p, TR and ig energy) and that also considers sandbar and dune dynamics is needed to fully understand and predict beach response. Despite having a detailed set of data with morphological and hydrodynamic characteristics, it remains difficult to provide a conclusive statement on the theoretical effect(s) of storm clustering. One might expect a depleted beach to be more prone to erosion but recent work (Yates et al., 2009) indicates the opposite: since beaches always tend to an equilibrium shape and since a storm tends to push the beach far from equilibrium, sequences of storms should be less and less effective in driving the beach away from equilibrium. Our results have elements that are consistent with the simple model of Yates et al. (2009) although we also suggest that other characteristics of the 'storm chronology' such as tidal stage and surfzone characteristics are at least as important as wave height and are needed in such a model in order for it to be more universally applicable. Eroded sediment, possibly transported in the offshore direction but not lost to deeper water could fundamentally alter the response to the following storms and give rise to a feedback involving the 'chronology' of waves, sediment transport and morphological change. Sediment mobilized from the beach and deposited in the surf zone has the potential to change the shape of the cross-shore profile, enhance wave dissipation (i.e. waves might begin to break further offshore) which in turn would feedback into sediment transport. Assessments of the morphodynamic effect of a 'cluster' or a 'chronology' of storms, and the ability to predict the dynamics related to beach recovery depend not only on the hydrodynamic characteristics of the storm but also need to account for beach type, the presence and location of subaqueous sandbars, spring-neap concurrence and beach vulnerability.

6. Conclusions

Analysis of observations from a detailed field campaign involving daily beach surveys over a wide area shows large variability in cross-shore and alongshore beach response to a sequence of storms. Larger scale bathymetric surveys indicate the presence of pronounced 3D sandbar patterns at the beginning and the end of the campaign. The sequence/cluster of storms did not result in enhanced erosion as observed at other locations, because of the different characteristics of each storm and, possibly, because the largest storm occurred at the beginning of the sequence. The response to each storm is difficult to anticipate especially because of the interplay between water levels, angle of wave approach, amount of infragravity energy and pre-existing beachface conditions. Multiple regression analysis indicates that the coupled effect of offshore hydrodynamic variables and ig energy in the inner surf zone can explain at least part of the changes occurring over the beachface.

The findings are of critical importance in improving the understanding and prediction of beach response to storms. The interplay between offshore wave characteristics, their transformation across the surf zone and pre-existing bathymetry remains difficult to disentangle but our results clearly show that it is this complex interplay, rather than the direct control of wave energy, that controls the response to storms. These observations also provide a valuable dataset with which to test advances in numerical modelling and how increased process knowledge can lead to improved predictions in nearshore morphodynamics.

Acknowledgments

We wish to thank all the organizations that have provided financial support for the field experiment, in particular the French DGA (ECORS project). GC was funded by the NZ-FRST, the French Embassy in New Zealand, CNRS (France), and Cantabria Campus Internacional (Augusto Gonzalez Linares Program). JM and JB, and the surf zone field measurements were funded by NSF# OCE# 0728324. Thanks to the two anonymous referees for their constructive comments and suggestions.

References

Aagaard, T., Kroon, A., Andersen, S., Sorensen, R.M., Quartel, S., Vinther, N., 2005. Intertidal beach change during storm conditions; Egmond, The Netherlands. Mar. Geol. 218, 65–80.

Almar, R., Castelle, B., Ruessink, B.G., Senechal, N., Bonneton, P., Marieu, V., 2010. Two- and three-dimensional sand-bar system behaviour under intense wave forcing and a meso-macro tidal range. Cont. Shelf Res. 30, 781–792. http://dx.doi.org/10.1016/j.csr.2010.02.001.

Almeida, L.P., Vousdoukas, M.V., Ferreira, Ó., Rodrigues, B.A., Matias, A., 2012. Thresholds for storm impacts on an exposed sandy coastal area in southern Portugal. Geomorphology 143–144, 3–12. http://dx.doi.org/10.1016/j.geomorph.2011.04.047.

Anderson, T.R., Frazer, L.N., Fletcher, C.H., 2010. Transient and persistent shoreline change from a storm. Geophys. Res. Lett. 37, L08401. http://dx.doi.org/10.1029/2009GL042252.

Battjes, J.A., 1974. Surf similarity. Paper presented at 14th Coastal Engineering Conference. Am. Soc. of Civ. Eng., Copenhagen.

Bird, E.C.F., 1985. Coastline Changes. Wiley & Sons, New York (219 pp.).

Birkemeier, W.A., 1979. The effects of the 19 December 1977 coastal storm on beaches in North Carolina and New Jersey. Shore Beach 47, 7–15.
Birkemeier, W.A., Nicholls, R.J., Lee, G.H., 1999. Storms, storm groups and nearshore morphologic change. Proceedings of the Coastal Sediments'99 Conference. ASCE, pp. 1109–1122.
Butel, R., Dupuis, H., Bonneton, P., 2002. Spatial variability of wave conditions on the French Atlantic coast using in-situ data. J. Coast. Res. SI36, 96–108.
Castelle, B., Bonneton, P., Dupuis, H., Senechal, N., 2007. Double bar beach dynamics on the high-energy meco-macrotidal French Aquitanian Coast: a review. Mar. Geol. 245, 141–159. http://dx.doi.org/10.1016/j.margeo.2007.06.001.
Castelle, B., Ruessink, B.G., Bonneton, P., Marieu, V., Bruneau, N., Price, T.D., 2010. Coupling mechanisms in double sandbar systems. Part 1: patterns and physical explanation. Earth Surf. Process. Landforms 35, 476–486. http://dx.doi.org/10.1002/esp.192.
Ferreira, O., 2005. Storm groups versus extreme single storms: predicted erosion and management consequences. J. Coast. Res. SI42, 221–227.
Ferreira, O., 2006. The role of storm groups in the erosion of sandy coasts. Earth Surf. Process. Landforms 31, 1058–1060. http://dx.doi.org/10.1002/esp.1378.
Frihy, O.E., Komar, P.D., 1993. Long-term shoreline changes and the concentration of heavy minerals in beach sands of the Nile Delta, Egypt. Mar. Geol. 115, 253–261.
Gallagher, E.L., Elgar, S., Guza, R.T., 1998. Observations of sand bar evolution on a natural beach. J. Geophys. Res. 103 (C2), 3203–3215.
Komar, P.D., 1998. Beach processes and sedimentation. Prentice Hall, Englewood Cliffs, N.J.
Le Cozannet, G., Lecacheux, S., Delvallee, E., Desramaut, N., Oliveros, C., Pedreros, R., 2011. Teleconnection pattern influence on sea-wave climate in the Bay of Biscay. J. Clim. 24 (3), 641–652.
Lee, G., Nicholls, R.J., Birkemeier, W.A., 1998. Storm-induced profile variability of the beach-nearshore profile at Duck, North Carolina, U.S.A.,1981–1991. Mar. Geol. 148, 163–177.
Masselink, G., Russell, P., Turner, I., Blenkinsopp, C., 2009. Net sediment transport and morphological change in the swash zone of a high-energy sandy beach from swash event to tidal cycle time scales. Mar. Geol. 267, 18–35.
Parisot, J.P., Capo, S., Castelle, B., Bujan, S., Moreau, J., Gervais, M., Réjas, A., Hanquiez, V., Almar, R., Marieu, V., Gaunet, J., Gluard, L., George, I., Nahon, A., Dehouck, A., Certain, R., Barthe, P., Ardhuin, F., Le Gall, F., Bernardi, P.J., Le Roy, R., Pedreros, R., Delattre, M., Senechal, N., MacMahan, J., 2009. Treatment of topographic and bathymetric data acquired at the Truc-Vert Beach during the ECORS Field Experiment. J. Coast. Res. SI56, 1786–1790.
Plant, N.G., Holland, K.T., Holman, R.A., 2006. A dynamical attractor governs beach response to storms. Geophys. Res. Lett. 33, L17607. http://dx.doi.org/10.1029/2006GL027105.
Ruessink, B.G., Coco, G., Ranasinghe, R., Turner, I.L., 2007. Coupled and noncoupled behavior of three-dimensional morphological patterns in a double sandbar system. J. Geophys. Res. 112 (C7). http://dx.doi.org/10.1029/2006JC003799.
Russell, P.E., 1993. Mechanisms for beach erosion during storms. Cont. Shelf Res. 13, 1243–1265.
Senechal, N., Gouriou, T., Castelle, B., Parisot, J.-P., Capo, S., Bujan, S., Howa, H., 2009. Morphodynamic response of a meso- to macro-tidal intermediate beach based on a long-term data set. Geomorphology 107, 263–274. http://dx.doi.org/10.1016/j.geomorph.2008.12.016.
Senechal, N., Abadie, S., Gallagher, E., MacMahan, J., Masselink, G., Michallet, H., Reniers, A., Ruessink, G., Russell, P., Sous, D., Turner, I., Ardhuin, F., Bonneton, P., Bujan, S., Capo, S., Certain, R., Pedreros, R., Garlan, T., 2011a. The ECORS-Truc Vert'08 nearshore field experiment: presentation of a three-dimensional morphologic system in a macro-tidal environment during consecutive extreme storm conditions. Ocean Dyn. 61, 2073–2098. http://dx.doi.org/10.1007/s10236-011-0472-x.
Senechal, N., Coco, G., Bryan, K.R., Holman, R.A., 2011b. Wave runup during extreme storm conditions. J. Geophys. Res. 116, C07032. http://dx.doi.org/10.1029/2010JC006819.
Southgate, H.N., 1995. The effects of wave chronology on medium and long term coastal morphology. Coast. Eng. 26, 251–270.
Stive, M., 2004. How important is global warming for coastal erosion? Clim. Chang. 64, 27–39. http://dx.doi.org/10.1023/B:CLIM.0000024785.91858.1d.
Thom, B.G., Hall, W., 1991. Behaviour of beach profiles during accretion and erosion dominated periods. Earth Surf. Process. Landforms 16, 113–127.
Van Enckevort, I.M.J., Ruessink, B.G., Coco, G., Suzuki, K., Turner, I.L., Plant, N.G., Holman, R.A., 2004. Observations of nearshore crescentic sandbars. J. Geophys. Res. 109, C06028. http://dx.doi.org/10.1029/2003JC002214.
Wang, P., Kirby, J.H., Haber, J.D., Horwitz, M.H., Knorr, P.O., Krock, J.R., 2006. Morphological and sedimentological impacts of hurricane Ivan and immediate post-storm beach recovery along the Northwestern Florida barrier-island coasts. J. Coast. Res. 6, 1382–1402.
Wright, L.D., Short, A.D., 1984. Morphodynamic variability of surf zones and beaches: a synthesis. Mar. Geol. 56, 93–118.
Yates, M.L., Guza, R.T., O'Reilly, W.C., 2009. Equilibrium shoreline response: observations and modelling. J. Geophys. Res. 114, C09014. http://dx.doi.org/10.1029/2009JC005359.
Zhang, K., Douglas, B.C., Leatherman, S.P., 2002. Do storms cause long-term beach erosion along the US East Barrier Coast? J. Geol. 110, 493–502.
Zhang, K., Douglas, B.C., Leatherman, S.P., 2004. Global warming and coastal erosion. Clim. Chang. 64, 41–58. http://dx.doi.org/10.1023/B:CLIM.0000024690.32682.48.

Please cite this article as: Coco, G., et al., Beach response to a sequence of extreme storms, Geomorphology (2013), http://dx.doi.org/10.1016/j.geomorph.2013.08.028